



# Development of mechanical soil stability in an initial homogeneous loam and sand planted with two maize (*Zea mays* L.) genotypes with contrasting root hair attributes under *in-situ* field conditions

U. Roskopf<sup>1</sup> · D. Uteau<sup>2</sup> · S. Peth<sup>1</sup>

Received: 20 December 2021 / Accepted: 20 June 2022 / Published online: 25 June 2022  
© The Author(s) 2022

## Abstract

**Purpose** Soil structure evolving from physical and biological processes is closely related to soil mechanical characteristics and texture. We studied the influence of substrate and genotype on the initial development of mechanical traits, differences between depths, and changes over the course of two years in the field.

**Methods** Plots were homogeneously filled with a loam and a sand and planted with two maize (*Zea mays* L.) genotypes (wild type (WT) and *rth3* mutant) with contrasting root hair attributes. Undisturbed soil cores were taken in 2019 and 2020 at 14 and 34 cm depth. Confined uniaxial compression tests were performed to determine pre-compression stress ( $\sigma_{pc}$ ), compressibility ( $C_c$ ,  $C_s$ ) and elasticity index (EI).

Mechanical energy was calculated based on penetration resistance (PR) tests with a penetrometer needle resembling root geometries.

**Results**  $\sigma_{pc}$ ,  $C_c$  and  $C_s$  were significantly higher in loam as compared to sand, whereas the factor genotype proved to be negligible. Over time,  $\sigma_{pc}$  increased and  $C_c$  decreased in loam from 2019 to 2020 and  $C_s$  declined in both substrates. Higher mechanical energies were observed in loam and partially in WT. Required energy was higher at 14 cm than at 34 cm depth and decreased from 2019 to 2020 in sand. Air-dry sand samples required four times as much energy than those at matric potential ( $\Psi_m$ ) of -50 kPa.

**Conclusion** For the development of the mechanical traits examined texture proved to be the dominating factor and changes in soil stability could be observed within a short period of time.

Responsible Editor: Doris Vetterlein.

**Supplementary Information** The online version contains supplementary material available at <https://doi.org/10.1007/s11104-022-05572-5>.

U. Roskopf (✉) · S. Peth  
Institute of Soil Science (Soil Biophysics Group),  
Leibniz Universität Hannover, Herrenhäuser Str. 2,  
30419 Hannover, Germany  
e-mail: rosskopf@ifbk.uni-hannover.de

D. Uteau  
Department of Soil Science, Faculty of Organic  
Agricultural Sciences, University of Kassel,  
Nordbahnhofstr. 1a, 37213 Witzenhausen, Germany

**Keywords** Compression index · swelling index · soil elasticity · soil mechanical stability · penetration resistance · pre-compression stress

## Abbreviations

$C_c$	Compression index
$C_s$	Swelling index
EI	Elasticity index
$\varepsilon$	Void ratio
$R^2$	Coefficient of determination
<i>rth3</i>	Maize mutant with suppressed root hair elongation
$\rho_b$	Bulk density

$\sigma_{pc}$	Pre-compression stress
PR	Penetration resistance
WT	Maize wild type
$\Psi_m$	Matric potential

## INTRODUCTION

Soil mechanical characteristics evolve from the interplay of texture and structure of a soil, structure itself being influenced by a variety of biological, physical, and chemical factors (Bacq-Labreuil et al. 2019; Bryk et al. 2017; Grosbellet et al. 2011; Hallett et al. 2009; Naveed et al. 2014; Schon et al. 2017). Root growth constitutes a major biological factor for the formation of soil structure and depends on the plant's characteristics and the prevailing environmental conditions. Structural changes take place over time and are accompanied by the evolution of the mechanical properties of the soil. This development can be expected to be considerably different in the field compared to controlled lab conditions.

How root growth re-organises the pore system and aggregate size distribution, largely depends on soil texture. Bacq-Labreuil et al. (2019) showed that phacelia (*Phacelia tanacetifolia* Benth.) decreased soil porosity in a sandy loam as compared to the unplanted control but did not alter porosity of a clayey soil. The changes in bulk density ( $\rho_b$ ) induced by root growth are mainly determined by soil structure and particle size. When roots grow in homogeneous soil, particles are rearranged, whilst in a more structured soil the existing pore space is utilized (Phalempin et al. 2021). Growth of coarse roots increase macropores, whereas finer roots display a high flexibility and improve micro-porosity (Bodner et al. 2014). Roots do not only greatly contribute to the creation of biopores but also improve connectivity of the pore system (Lucas et al. 2021). Furthermore, they have an influence on soil aggregation. In an agriculturally reclaimed mining area, macro-aggregate size distribution remained similar throughout the 24 years reclamation age (Pihlap et al. 2019), whereas aggregates <1000  $\mu\text{m}$  increased in a clay through phacelia growth (Bacq-Labreuil et al. 2019).

Mucilage released at the root tip (Oleghe et al. 2017; Naveed et al. 2017) and an intact root tip (Iijima et al. 2004; Bengough and McKenzie 1997) ease the roots' way through the soil. The rhizosphere

provides a habitat for soil microorganisms and root exudates have a major impact on bacterial community structure in the rhizosphere (Haichar et al. 2008). Roots contribute indirectly to soil structural evolution even after the plant's death, by providing nutrient and carbon to soil organisms (Li et al. 2015; Pett-Ridge and Firestone 2017), increasing both functional and taxonomic diversity through root detritus (Nuccio et al. 2020) and altering microbial activity through the spatial organisation of the pore network (Nunan et al. 2017). Furthermore, former root channels constitute an important root growth pathway in soil layers with a high mechanical impedance (Han et al. 2015). Both root exudates (Burak et al. 2021; Galloway et al. 2020) and existence of root hairs (Carminati et al. 2017) contribute to the formation of a rhizosheath, which in turn can stabilize soil (Wang et al. 2017) and affect both porosity and connectivity of the surrounding pores (Koebernick et al. 2017). In the light of these processes plant growth affects soil structure formation and stabilization by a wide range of interacting mechanisms, which in turn ultimately influences soil mechanical parameters. Roots may encounter layers which they are not able to penetrate, unfavourable mechanical conditions being a possible reason for that. For instance, Bengough et al. (2011) mentioned penetration resistances (PR) of 2 MPa reducing root elongation rates in maize by 50% compared to non-impeded roots.

It is a combination of both abiotic and biotic factors that influences structure formation in a soil (Barto et al. 2010), oftentimes it is difficult to distinguish between them (Oades 1993). Physical factors such as climatic conditions and weather, influence soil structural development directly by freezing and thawing or swelling and shrinking cycles and indirectly through affecting plant growth. Root systems with finer roots can dry out the soil locally leading to cracks (Oades 1993), whereas larger roots can create macropores or use existing macropores to reach deeper soil regions (Lucas et al. 2019) in search of water and nutrients.

Leuther and Schlüter (2021) examined the impact of freezing and thawing cycles on soil structure and found that even only two of these cycles might already lead to a fragmentation of soil clods and an increase of unsaturated hydraulic conductivity. Wetting and drying leads to swelling and shrinking processes in the soil which affect macro- and mesoporosity and greatly depend on clay content and

mineralogy (Diel et al. 2019). Stronger organic bonds leading to an increase in macroaggregates and their stability, can be expected between 2:1 clay minerals compared to a soil in which 1:1 clay minerals dominate (Denef and Six 2005). In managed grasslands Barto et al. (2010) showed that a higher percentage of sand in a soil interferes with soil aggregation.

The experimental site we examined consisted of plots that were homogeneously filled with two defined substrates and planted with two maize genotypes (Vetterlein et al. 2021). This set-up gave us the unique opportunity to study the development of soil mechanical properties following an initial homogeneous state under field conditions. The aim of this study was to quantify the effect of the factors substrate and genotype on soil stability, compressibility, elasticity, and mechanical energy required for root growth and to describe their spatial and temporal development.

The two genotypes employed in the experiment differ in their capability to form root hairs. The wild type (WT) forms root hairs, whereas in the *rth3* mutant their elongation is suppressed. Root hairs play a central role in the cohesion between roots and soil particles (De Baets et al. 2020) and might therefore lead to higher stabilisation. However, differences in root length densities between genotypes might have a greater effect on soil mechanical properties than the actual root hairs. The samples in this study were taken between rows of maize due to spatial limitations. We hypothesized substrate to be the driving factor with higher stability and compressibility expected in loam as the higher clay content promotes soil aggregation thus enhancing soil stability. Bronick and Lal (2005) describe the important role of clay in the formation of compound particles that contribute greatly to soil aggregation. Shrinking and swelling processes in soils containing clay are crucial in soil structure formation (Dixon 1991). Higher clay contents and a greater level of aggregation in loam bring about a higher initial void ratio ( $\epsilon$ ) and its more pronounced decline when stresses exceed pre-compression stress ( $\sigma_{pc}$ ) (Lebert and Horn 1991). The sand on the other hand is a single-grain substrate with weak cohesion between particles (Lebert and Horn 1991), less potential for aggregation and a pronounced primary pore system that leaves little room for compression.

Concerning the development over time and space, we expect  $\sigma_{pc}$  to be higher closer to the soil surface, caused by the influence of environmental conditions,

mainly drying and re-wetting. As structural development takes time,  $\sigma_{pc}$  as a measure of stability is likely to increase from one year to the next and compressibility (compression index  $C_c$  and swelling index  $C_s$ ) is expected to decrease. Regarding PR, we predict higher values in loam compared to sand and a possible influence of genotype relating to their root system. We further hypothesize the heterogeneity to be greater at 14 cm depth and to increase with time due to the development of soil structure, all in all leading to higher values in the second year. Our overall hypothesis is, that in sand changes in mechanical characteristics caused by processes of structural formation will be less pronounced than in a loam.

## MATERIALS AND METHODS

### Soil plot experiment

The soil plot experiment was established in October and November 2018 in the framework of the DFG priority programme 2089 “Rhizosphere Spatiotemporal Organisation - a key to rhizosphere functions”. It constitutes a new approach of studying the development of soil mechanical stability parameters. The site is located at the experimental station of the Helmholtz Centre for Environmental Research in Bad Lauchstädt in Germany (N 51° 23.425440, E 11° 52.555980). Field plots were excavated and filled with two homogeneous substrates, a loam and a sand (loam: 32.5% sand, 47.9% silt, 19.5% clay; sand: 91.8% sand, 5.6% silt, 2.6% clay (Vetterlein et al. 2021)), and planted with maize genotypes WT and *rth3*. The randomized block design consisted of six plots for each combination of texture and genotype, resulting in six field replicates. Fertilization ensured an equal supply with nutrients in both substrates. Maize was first sown in April 2019. Details regarding the experimental set-up including filling of field plots, fertilization, and agronomic measurements are described in Vetterlein et al. (2021).

### Sampling and sample preparation

Two sets of undisturbed soil cores were taken at growth stage BBCH83 (early dough) (Meier and Biologische Bundesanstalt für Land- und Forstwirtschaft 1997) in 2019 and 2020, one for a confined uniaxial

compression test, the other for PR measurements. For the compression tests, cylinders with a diameter of 10 cm and a height of 3 cm were employed, resulting in a ratio of diameter to height of 3.33, which is in accordance with the International Organization for Standardization (ISO 2017), whereas for the remainder of the experiments cylinders with a diameter of 10 cm and a height of 6 cm were utilized, giving enough room for PR measurements. Samples were taken at a specific location in each field plot at two different depths (14 cm and 34 cm upper cylinder edge) and stored in the dark at 4°C until further use. The sample location was between rows of maize with a distance of 22 cm to the next plant. The position was in close proximity to the location used for root sampling in Vetterlein et al. (2022) who took soil cores 10 cm from the foot of the maize plant. In preparation for the measurements, samples were saturated with tap water and subsequently put on ceramic suction plates until weight consistency was reached to obtain the desired matric potentials ( $\Psi_m$ ) at the start of the measurements. These were -50 kPa  $\Psi_m$  for the uniaxial compression test and a sequence of -3, -12.5 and -50 kPa  $\Psi_m$  for the PR with an additional airdry step for sand in 2020. Note that the unit kPa is used both for the stress and for  $\Psi_m$ , for which we explicitly stated “kPa  $\Psi_m$ ” to avoid confusion.

#### Confined uniaxial compression test

Undisturbed soil samples were measured at  $\Psi_m$  -50 kPa with an oedometer (fig. 1; Eijkelcamp 08.67 Compression test apparatus, Giesbeek, Netherlands) and the software Physical soil test Version 2.0.4 (Eijkelcamp, Giesbeek, Netherlands) to obtain information on pre-compression stress ( $\sigma_{pc}$ ), compression indices ( $C_c$ ), swelling indices ( $C_s$ ), and elasticity indices (EI). The basic idea of the oedometer tests is to load a soil sample confined in a cylinder with a defined pressure and measure the settlement in vertical direction. Above and below the built-in soil sample are sintered metallic plates through which water can flow that is pressed out of the pores. The oedometer is furthermore equipped with a tensiometer to allow measurement of  $\Psi_m$  throughout the experiment. In order to level out any irregularities at the sample surface, the device exerted a pre-pressure of 5 kPa for 20 s, which we defined as the actual start of the test. This was followed by 11 log-equidistant loading steps

ranging from 10 to 575 kPa and a final unloading step of 5 kPa. The duration of each step was 20 min for loam and 5 min for sand to account for different consolidation times of these substrates and was established in a pre-test prior to the experiment. Applied stress, vertical settlement and  $\Psi_m$  were logged every 2 s. For the necessary calculations bulk density ( $\rho_b$ ) was determined by drying the soil cores at 105°C for 48 h after measurements; particle density (loam 2.46 g cm<sup>-3</sup> and sand 2.62 g cm<sup>-3</sup>, Roskopf et al. 2022) had been quantified at an earlier stage.

A typical stress-strain curve (Fig. 1b) shows the settlement behaviour of a soil subjected to a series of successively increasing vertical loads and generally consists of a recompression range and a virgin compression range. Vertical stress is registered in kPa,

$$\sigma = \frac{F}{A_{cylinder}}$$

where F is the vertical force applied and A the cross-sectional area of the soil sample. The settlement is reflected in the void ratio  $\varepsilon$ , namely:

$$\varepsilon = \frac{V_{pores}}{V_{solids}}$$

The first part of the curve is the so-called recompression range, as the soil already had been exposed to stresses in this order of magnitude in the past. Its slope is defined as  $C_s$ :

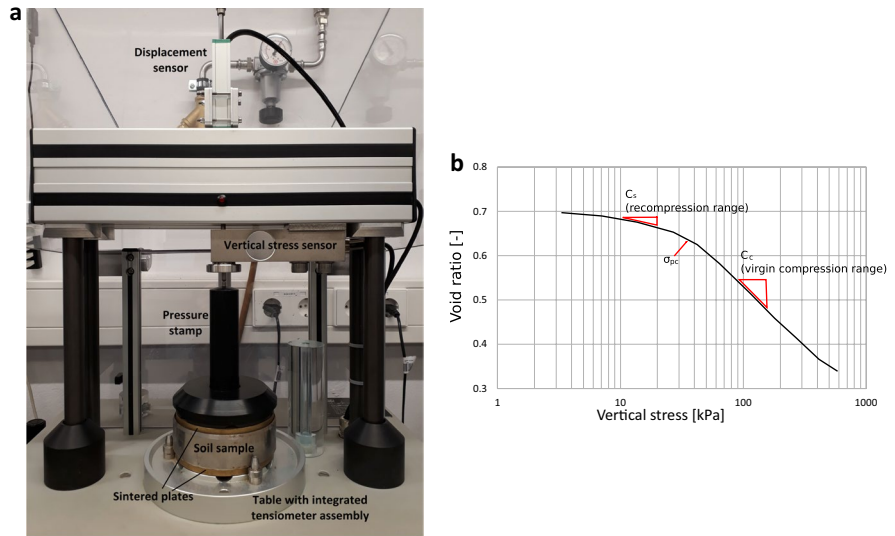
$$C_s = \frac{\Delta\varepsilon_{recompression\ range}}{\Delta\log\sigma_{recompression\ range}}$$

Evaluation of  $\sigma_{pc}$  was based on the methods of Casagrande (1936) and the logistic function suggested by Gregory et al. (2006). The slope of the virgin compression range (Fig. 1b) is called  $C_c$ , which was calculated analogously to  $C_s$ :

$$C_c = \frac{\Delta\varepsilon_{virgin\ compression\ range}}{\Delta\log\sigma_{virgin\ compression\ range}}$$

The expression “virgin compression range” emphasizes the fact that the soil has not previously been subjected to pressures to this extent. The EI was calculated for the final loading step of 575 kPa with

**Fig. 1 a** Uniaxial confined compression device with built-in soil sample. **b** Schematic stress-strain relationship indicating pre-compression stress ( $\sigma_{pc}$ ), swelling index ( $C_s$ ) as the slope of the recompression range and compression index ( $C_c$ ) as the slope of the virgin compression range



$$EI = \frac{\Delta \epsilon_{rebound}}{\Delta \epsilon_{loaded}}$$

as used by Peth et al. (2010). The ratio ranges from 0 (completely plastic behaviour) to 1 (completely elastic behaviour).

Penetration resistance experiment

For the PR experiment a stainless-steel cover was devised to ensure correct positioning of the tests with sufficient distance between penetration sites and cylinder edge, and to prevent evaporation during the experiment, as only the hole in use was left uncovered. As the samples were sufficiently large to accommodate 12 penetrations, the experiment was performed at three different  $\Psi_m$  (-3, -12.5, and -50 kPa  $\Psi_m$  and an additional air-dry step in 2020) with three replicates per cylinder. For air-drying, samples were placed on a wire mesh and put underneath a fume hood at room temperature until no further weight loss occurred. A material testing machine (100 kN Allround Table Top Zwick/Roell, Ulm, Germany) equipped with a sensitive microsensor with a nominal force of 10 N (accuracy grade 1 according to ISO 7500-1 (ISO 2018) down to 0.02 N), was employed to push a penetration needle at a constant rate of 120 mm h<sup>-1</sup> to a depth of 20 mm into the soil. The effect of the penetration rate on force measurements had been evaluated beforehand by comparing the forces resulting from real root growth velocities

to higher ones which are more practicable to apply in the lab (Roskopf et al. 2022). The results suggested that at a rate of 120 mm h<sup>-1</sup> the resulting forces can be regarded as representative for those obtained at real root growth rates. The penetrometer probe was non-recessed with a diameter of 1 mm (Oleghe et al. 2017) and a 15° semi-angle resembling root geometries (Ruiz et al. 2017). The use of a non-recessed shaft allowed us to retract the PR needle at insertion speed which was performed for one of the three replicate measurements per cylinder. Displacement and forces were logged every 10 μm. Results of three measurements per cylinder at each  $\Psi_m$  were averaged and corrected for shaft friction. PR was calculated as follows:

$$PR = \frac{F_{Z,m}}{A_{PR\ needle}}$$

with  $F_{Z,m}$  being the measured axial penetration force and  $A$  the cross-sectional area of the PR needle. To calculate the mechanical energy demand according to Ruiz et al. (2017), the following formula was employed:

$$U = \int_{0.002}^{0.018} F_{Z,m} dz$$

with  $dz$  representing the incremental length, and the limits of 2 and 18 mm chosen to guarantee full contact between the cone and the soil, with values for all replicates being available. Results were subsequently



related to the length of one metre. Samples were weighed after drying for 48 h at 105°C to calculate  $\rho_b$ .

### Statistical analysis

To test the effects of substrate and genotype and their interaction on the variables measured, data were sorted according to year and depth, and multi-factorial ANOVA was calculated after preconditions were verified. Where applicable, a subsequent Tukey HSD-test was performed. The same approach was applied to determine differences between depths and years. The energy data derived from PR measurements did not meet pre-requisites for ANOVA, so data transformations had to be carried out beforehand. For this purpose, data for the groups according to depth and year were log-transformed prior to ANOVA, subsequently significant differences for the factors substrate, genotype and their interaction within each  $\Psi_m$  were quantified. Airdry samples were analysed separately, as only sand values in 2020 were available. Here, one-factorial ANOVA was used to determine differences according to genotype and to substrate. Splitting the data into loam and sand we then calculated whether the factors depth and year caused any differences within energy values. For all tests,  $H_0$  was specified as no differences occurring between observation groups and the significance threshold ( $\alpha$ ) was set at 0.05. Statistical tests were executed with the open-source software RStudio version 1.3.1093 (RStudio Team 2020). Figures were prepared with R-package ggplot2 version 3.3.5 (Wickham 2016).

## RESULTS

### Effect of genotype and substrate on bulk soil mechanical parameters

Result tables for all parameters including mean values and standard errors for all groups can be found in the online resource (Table S1) alongside full ANOVA tables (Tables S2–S5). The impact of genotype and substrate on  $\sigma_{pc}$  is graphically presented in Fig. 2. At 34 cm in 2019 the only differences in  $\sigma_{pc}$  caused by the factor genotype (Fig. 2a;  $p=0.033$ ) with higher  $\sigma_{pc}$  values for *rth3* compared to WT and the only significant interaction ( $p=0.015$ ) between the two factors

(higher  $\sigma_{pc}$  for WT in loam and for *rth3* in sand; not shown). Values (omitting outliers) ranged from 19–52 kPa in loam and from 15–45 kPa in sand (Fig. 2c, d). Higher values in loam compared to sand were found in all groups apart from 34 cm in 2019 (Fig. 2c).

Compressibility was influenced by the factor substrate (Fig. 3), which led to strongly contrasting values with loam displaying a much higher compressibility than sand within the entire stress-strain relationship.  $C_c$  were significantly higher in loam in all groups (Fig. 3a, b), the same being true for  $C_s$  (Fig. 3c, d) (all  $p<0.001$ ; full statistical tables are included in the supplementary information). Both ranges and inter-quartile ranges of  $C_c$  in sand were remarkably low. In loam  $C_s$  values differed considerably according to depth and year, whereas values in sand were more similar to each other. Contrarily, neither  $C_c$  nor  $C_s$  indices were affected by the factor genotype (not shown). No interactions occurred in any of the compressibility statistics.

EI were considerably higher in sand with mean values of 0.120–0.129 as opposed to loam with mean values between 0.045 and 0.052 (not shown). P-values were below 0.001, see supplementary information for statistical details. Again, no influence of genotype on EI could be discerned.

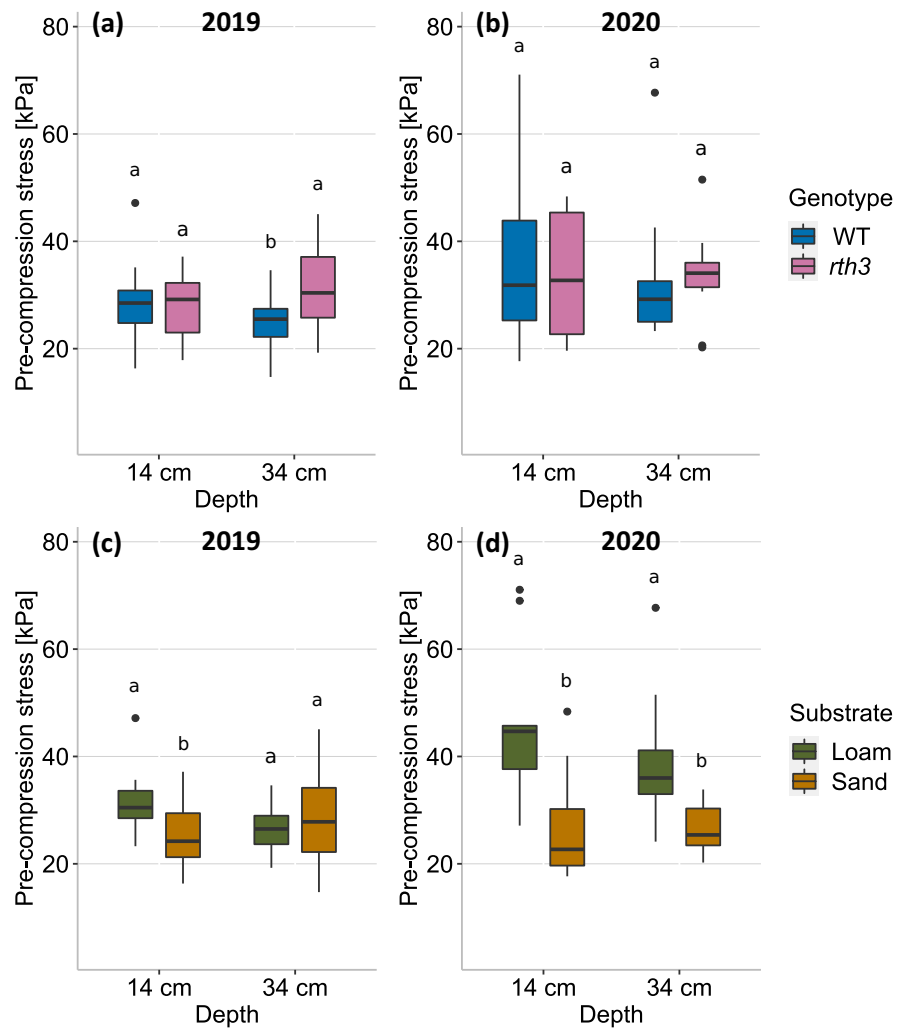
Significant correlations were observed in loam between  $\rho_b$  and  $\sigma_{pc}$  (Fig. 4a),  $C_c$  (Fig. 4b), and  $C_s$  (Fig. 4c).  $R^2$  decreased and p-values increased from one year to the next, especially for  $\sigma_{pc}$  the importance of  $\rho_b$  as an explanatory variable was diminished with time.  $\sigma_{pc}$  and  $C_c$  (Fig. 5a) or  $C_s$  (Fig. 5b), respectively, were negatively correlated (Fig. 5), whereas a positive relationship was found between  $C_s$  and  $C_c$  (Fig. 5c). Again, the same pattern occurred with strong relationships in 2019, and weaker and non-significant ones in 2020.

In sand the corresponding correlations were much weaker and mainly not significant (data not shown, see supplementary information S6).

### Effect of depth and year on bulk soil parameters

The influence of the factors depth and year was analysed here more specifically and is graphically presented in Figures 6, 7, 8, along with indication of statistical significance. Full statistical tables are included in the online resource (Tables S7–S11). In sand,  $\rho_b$  was significantly lower at 34 cm depth than

**Fig. 2** Effect of genotype (top) and substrate (bottom) on pre-compression stress. Data were grouped according to year and depth,  $n = 24$ . Significant differences are indicated by contrasting letters



at 14 cm (Fig. 6a), and the factor year did not result in significant differences (Fig. 6b). The opposite was the case in loam with similar values according to depth but significantly higher  $\rho_b$  in 2020 compared to 2019. In none of the treatments  $\sigma_{pc}$  (Fig. 7) were affected by depth, but it increased for both genotypes in loam from 2019 to 2020 (Fig. 7b).

Regarding the compressibility, depth did not influence  $C_c$  (Fig. 8a, b), and higher  $C_s$  values (Fig. 8c, d) were measured at 34 cm depth in loam, significantly for WT. Year turned out to be the dominant factor for changing soil stability leading to lower compressibility (tendency in  $C_c$  in L *rth3*) in loam in 2020 compared to 2019. In sand,  $C_c$  remained constant over depths and years with a remarkably low range. Lower

$C_s$  values in 2020 could also be observed in sand, albeit not significant for *rth3*.

#### Effect of genotype and substrate on energy required for root growth

Generally, the energy needed for one metre root growth increased with decreasing  $\Psi_m$ . To better understand the effect of the factors genotype and substrate, data were grouped according to depth and year, as these groups displayed distinct patterns. The factor genotype proved to be of minor relevance with significant differences in only two groups out of twelve (Fig. 9). Significantly higher energy values for WT roots were observed in 14 cm 2019 at  $\Psi_m$  -12.5 kPa

**Fig. 3** Compression (top) and swelling (bottom) indices as affected by substrate. Data were grouped according to year and depth, n = 24. Different letters indicate significant differences

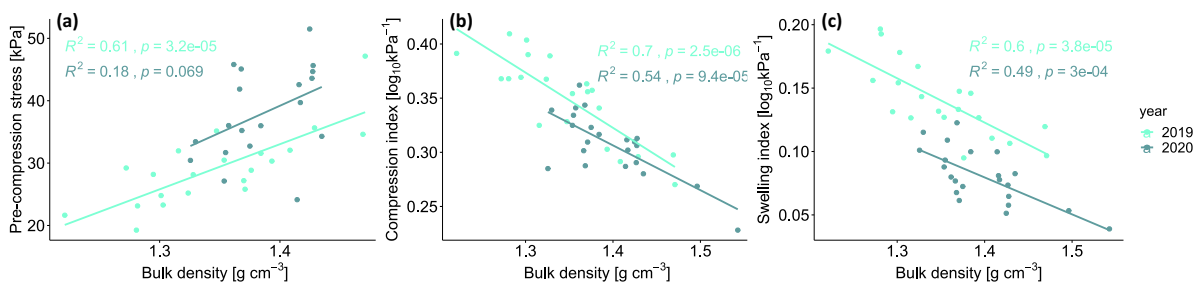
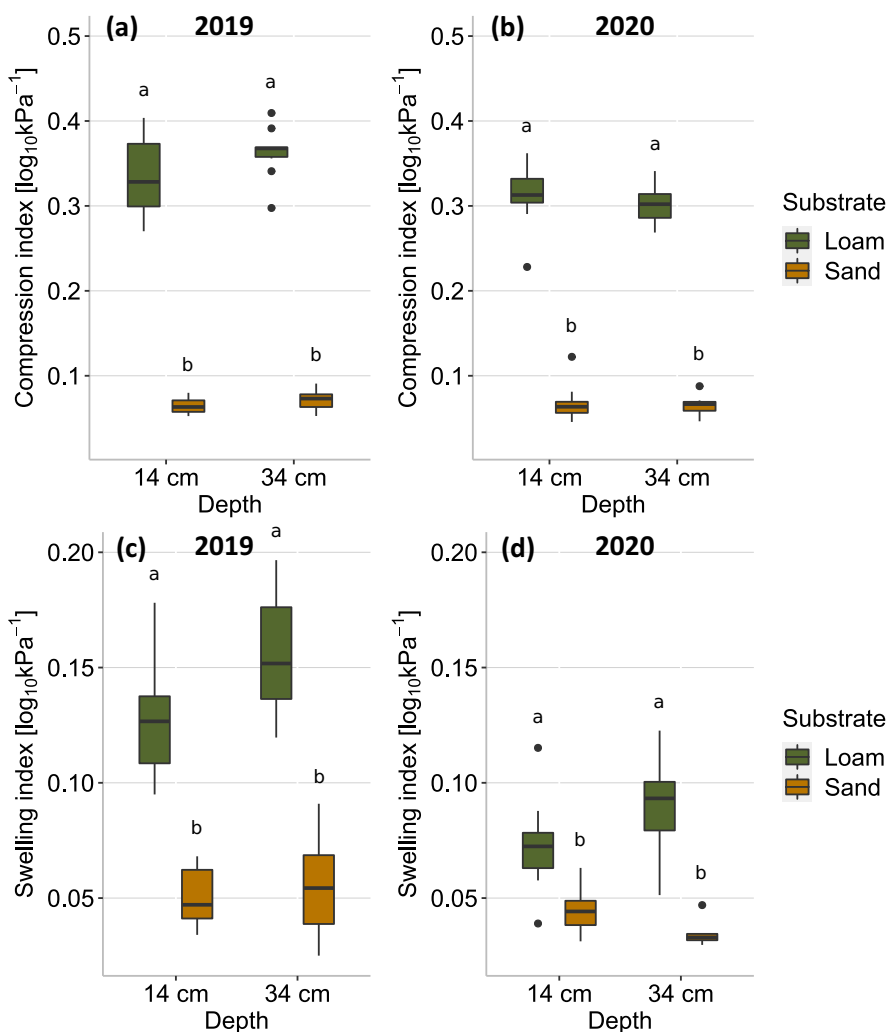


**Fig. 4** Correlations in loam between initial bulk density and pre-compression stress, compression index, and swelling index, respectively. Data were split according to year, n = 24.

In pre-compression data three outliers were removed. Coefficient of determination  $R^2$  and p-values are given



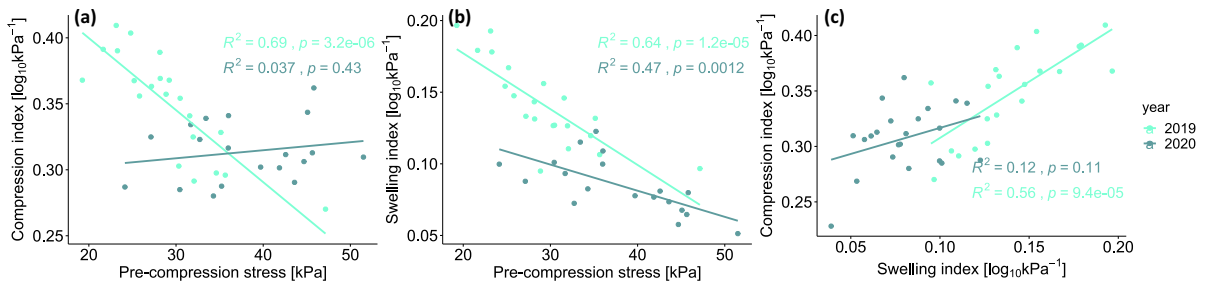


**Fig. 5** Correlations in loam between pre-compression stress, compression index, and swelling index, respectively. Data were separated by year, n = 23. Three outliers in pre-compression

stress were removed. Right graph shows correlation between swelling and compression indices. Coefficient of determination R<sup>2</sup> and p-values are indicated

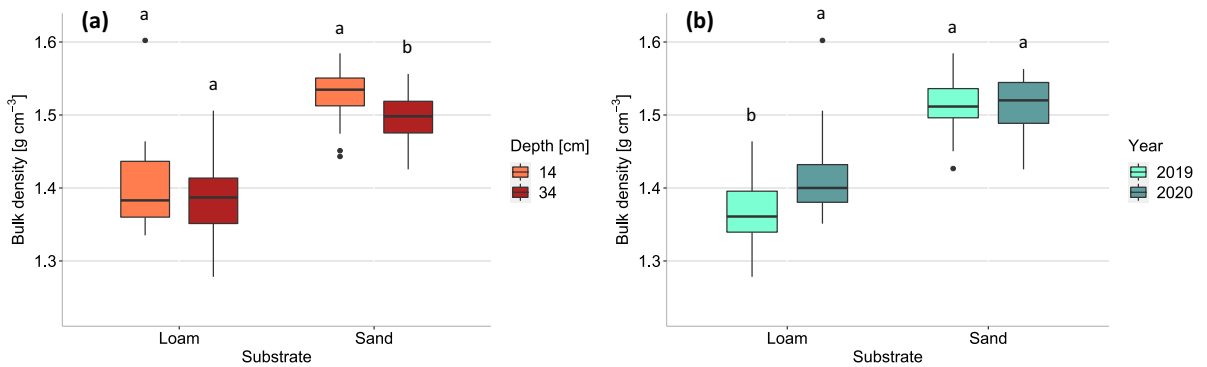


**Fig. 6** Bulk density in loam and sand according to the factors depth (left) and year (right), n = 48. Each value is a mean of two measurements. Significant differences are indicated by different letters

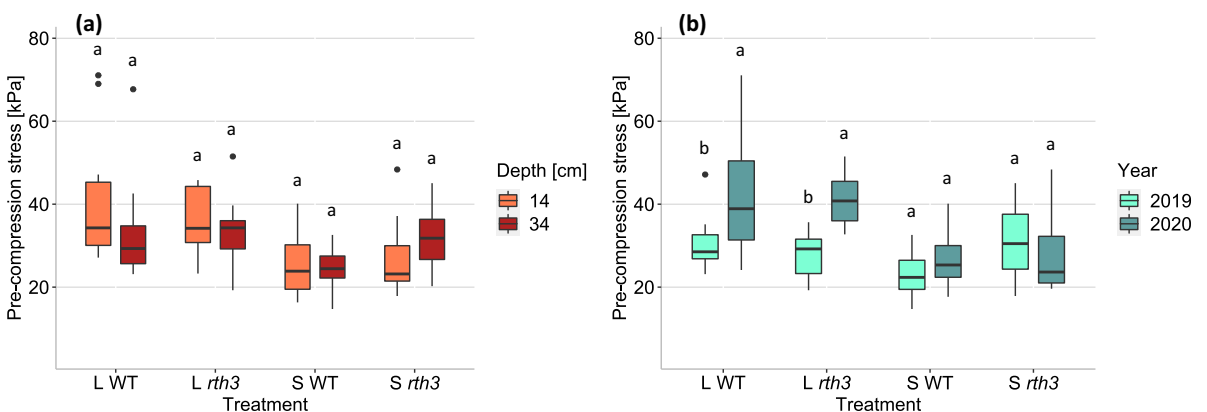


**Fig. 7** Pre-compression stress of the individual treatments (n = 24) L WT (loam wild type), L *rth3* (loam *rth3* mutant), S WT (sand wild type), and S *rth3* (sand *rth3* mutant) according

to the factors depth (left) and year (right), n = 24. Significant differences are indicated by different letters

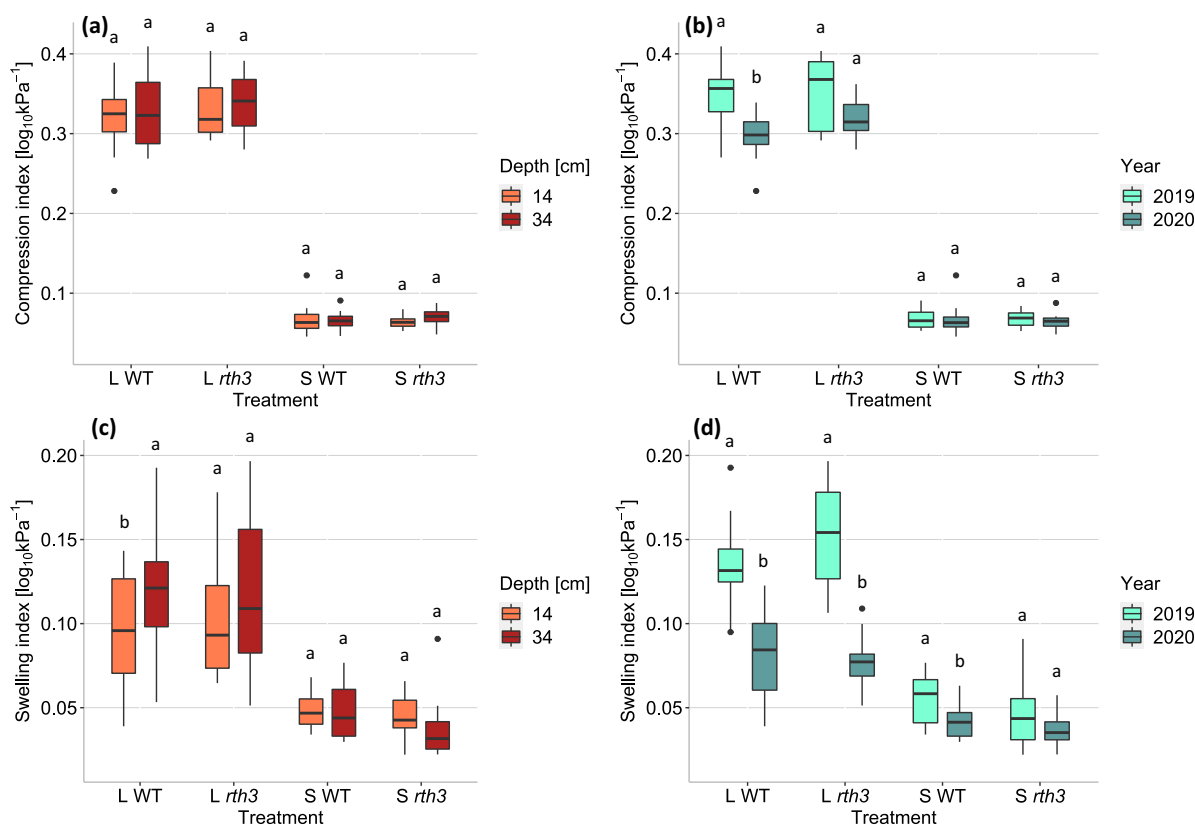


**Fig. 8** Compressibility of the individual treatments ( $n = 24$ ) L WT (loam wild type), L *rth3* (loam *rth3* mutant), S WT (sand wild type), and S *rth3* (sand *rth3* mutant) as affected by the factors depth (left) and time (right). The upper graphs display

the compression indices and the lower ones the swelling indices. Letters indicate differences according to the respective factor for each treatment

and in 34 cm 2020 at  $\Psi_m$  -50 kPa. No interactions between substrate and genotype could be observed.

Whereas in 2019 no significant differences occurred, in 2020 differences between energy values in loam and sand had developed in 14 cm at  $\Psi_m$  -50 kPa and in 34 cm depth at  $\Psi_m$  -12.5 and -50 kPa (Fig. 10b, d). Highest values of up to about 2 J (~2.5 MPa) were found at  $\Psi_m$  -50 kPa in loam. The samples from 34 cm depth in 2019 displayed the lowest range of values (Fig. 10c). The respective statistical table is S12.

Additional graphs depicting the course of the PR curves are located in the online resource (Figs. S1 and S2). In 2019 at 34 cm depth all treatments displayed similar curves. The most pronounced differences occurred at -50  $\Psi_m$  kPa in 2020 with loam WT being distinctly higher than loam *rth3* which in turn was higher than sand.

Effect of depth and year on energy required for root growth

When visually depicting the influence of the factors depth (Fig. 11a, c) and year on penetration energies (Fig. 11b, d) in loam and sand, a clear pattern becomes visible. At 14 cm depth values were higher in both substrates with significant differences for four out of six groups. Required energy in loam (Fig. 11b) remained constant over the years, whereas energy in sand (Fig. 11c) declined significantly from one year to the next. In loam an interaction between the factors occurred at  $\Psi_m$  -12.5 kPa ( $p = 0.0207$ ) with higher values at 14 cm depth compared to 34 cm in 2019 and vice versa in the following year. The inter-quartile range of both loam and sand values was reduced from one year to the next. ANOVA tables are available in the online resource (Table S13).

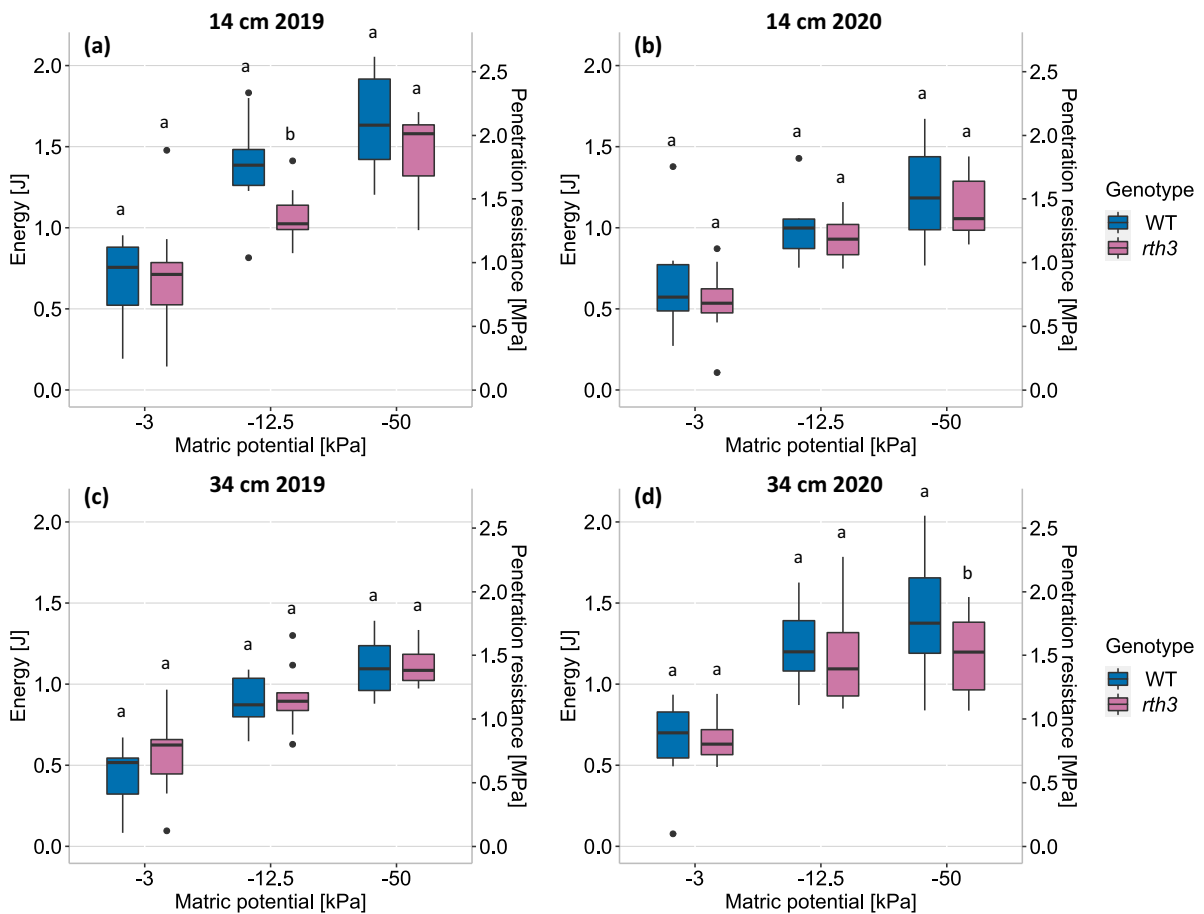


**Fig. 9** Energy required for a root of a defined maize genotype (WT = wild type, *rth3* = root hair-less mutant) with 1 mm diameter to grow 1 m. Data were grouped according to depth (14 and 34 cm) and year (2019 and 2020). Data were log-transformed for statistical analysis and subsequently rescaled to

the original data range for plotting. Measurements were taken at three matric potentials (-3, 12.5, and -50 kPa). Different letters within each matric potential ( $n = 24$ ) signify differences between genotypes

Due to technical limitations, measurements at air-dry conditions (not shown) could only be carried out in sand and only a few were done in loam, not enough to be analysed statistically. In sand, no differences caused by depth or genotype occurred. As the soil becomes drier, the plant must overcome much higher resistances and therefore invest more energy in root growth. In sand, PR of approximately 5 MPa were reached in both depths.

Regarding significant correlations between any of the other parameters with energy values, correlations could be observed between  $\rho_b$  and energy in sand at different  $\Psi_m$  (Fig. 12a, b, c). The respective correlations in loam were not significant and displayed no differences between years (data not shown). The

air-dry sand samples of 2020 did not significantly correlate with  $\rho_b$ .

## DISCUSSION

### Influence of genotype and substrate on bulk soil mechanical parameters

The bulk soil properties measured were not affected by genotype. Even examining the rhizosphere only, an influence of root hairs on  $\rho_b$  could be neither detected in barley (Koebernick et al. 2018) nor in maize (Phalempin et al. 2021). Roots play a crucial role in the formation of aggregates as they enmesh

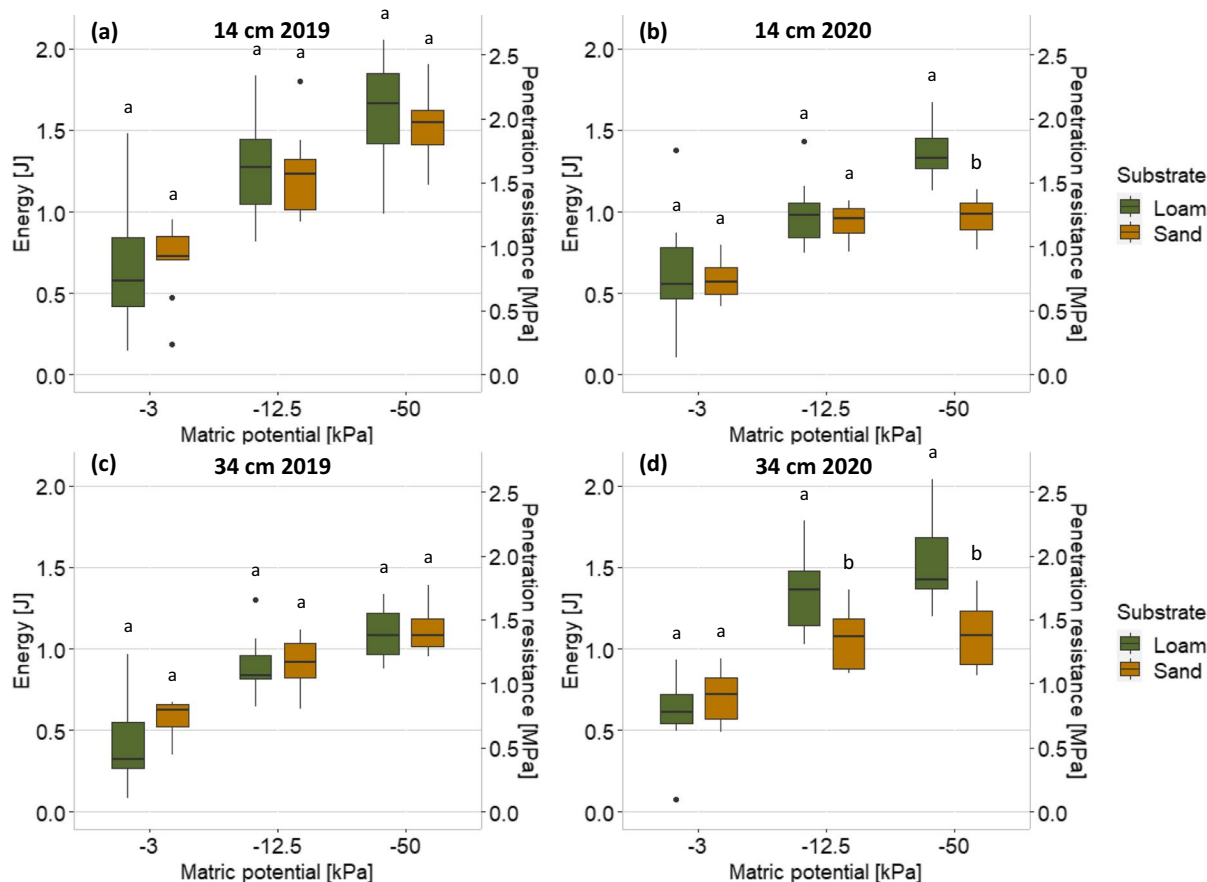


**Fig. 10** Energy required for a root with 1 mm diameter to grow 1 m in the respective substrate (loam and sand). Penetration resistance is displayed as secondary y-axis. Data were grouped according to depth (14 and 34 cm) and year (2019 and 2020). Data were log-transformed for statistical analysis and

subsequently rescaled to the original data range for plotting. Measurements were taken at three matric potentials. Different letters within each matric potential ( $n = 24$ ) signify differences between the substrates

particles and release organic compounds into the rhizosphere. Aggregates are stabilized by bacterial colonization and wetting-and-drying cycles, especially if clay particles are present (Bronick and Lal 2005). Kobernick et al. (2017 & 2018) concluded that barley root hairs have a stronger effect on the inter-aggregate pore space, creating a higher pore volume and increasing the percentage of small pores in the rhizosphere thus compensating for the compaction created by roots. These processes happen on a very local scale, possibly too small to be able to influence bulk soil measurements such as the ones in this study. Looking at root hairs and their influence on mechanical properties, especially

tensile strength, on the aggregate scale is a topic we aim to study at this site over the next years.

Geological history and mechanical loading are factors influencing  $\sigma_{pc}$  which can be ruled out in the present setup, because the plots were artificially filled and all use of machinery for agronomic measures was avoided, and the soil was not tilled. This provided us with a unique set-up to measure the development of soil mechanical parameters. Even though the samples in the present experiment were taken as undisturbed samples, they are – technically speaking – remoulded samples, as the plots were artificially packed with homogenized substrate. We drained all oedometer samples to  $\Psi_m$  -50 kPa to provide a comparable

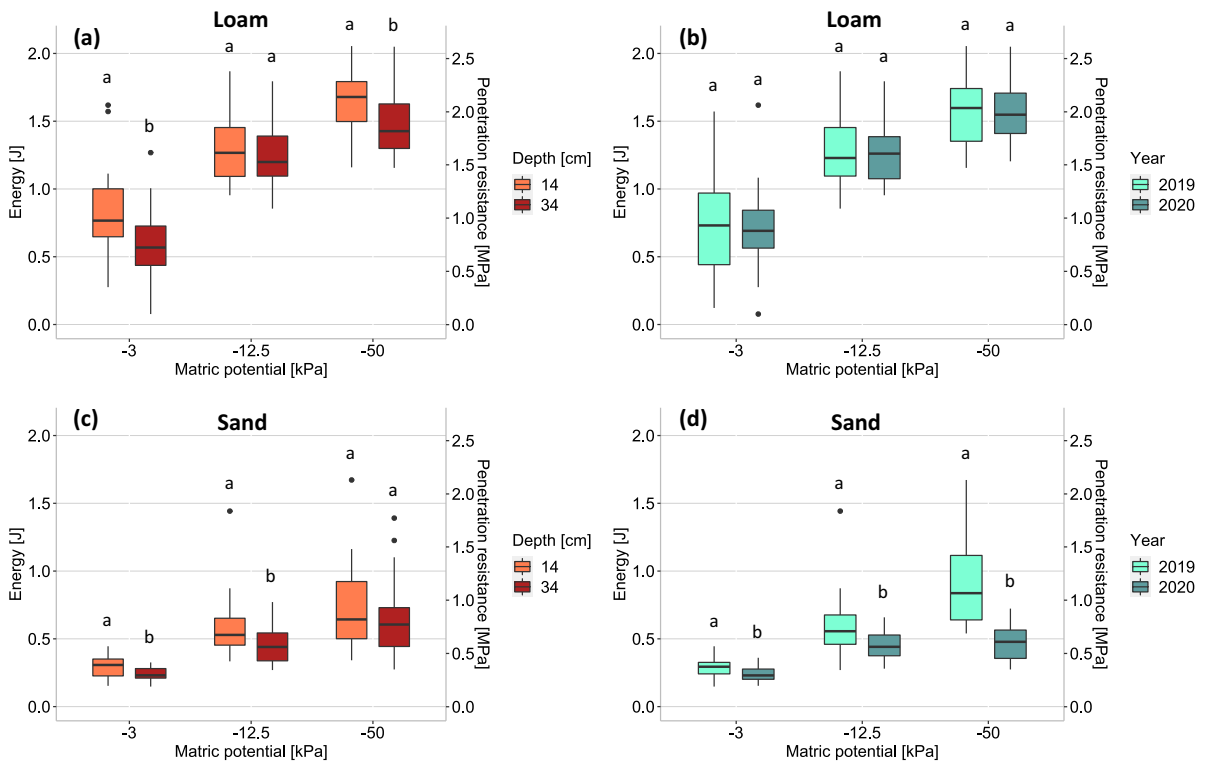


**Fig. 11** Energy needed for a 1 mm diameter root to grow 1 m in loam (top) and sand (bottom) as a function of depth (14 and 34 cm, left) and year (2019 and 2020, right), respectively.

Loam data were log-transformed prior to statistical analysis and were rescaled to the original scale for plotting. Significant differences are indicated for each matric potential, n =24

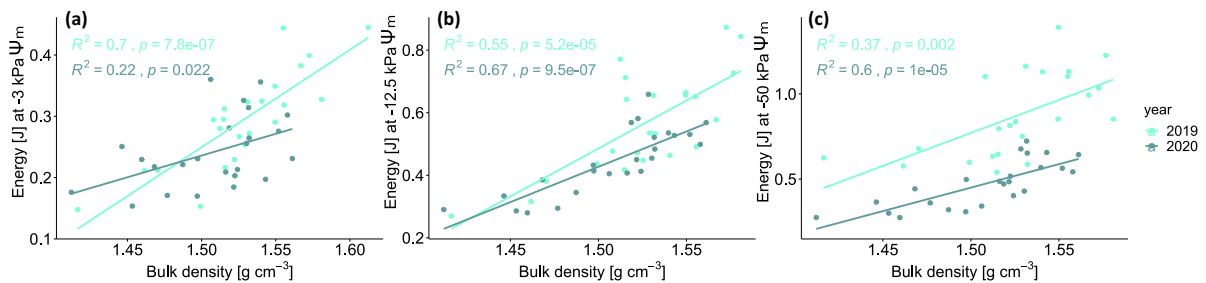


**Fig. 12** Correlations between bulk density and energy at matric potentials of -3, -12.5, and -50 kPa in sand, data were split by year, n = 24. Coefficient of determination R<sup>2</sup> and respective p-values are given

starting point for our measurements (Figures 2, 3, 4, 5, 6, 7, 8). In the present experiment the factor substrate had a major impact on  $\sigma_{pc}$  with higher values in loam compared to sand. This is in accordance with our hypothesis, as pronounced aggregation in loam leads to increased mechanical soil strength (Horn et al. 1994), especially at clay contents of more than 15% (Lebert and Horn 1991) which was the case for

the loam used. Soil strength is a function of forces between particles, interparticle friction and cohesion as well as the number of particle contacts per volume. In a single grain structure as for sand, the number of particle contacts and the forces between particles are much lower compared to a loam with a variety of particles sizes (Lebert and Horn 1991). Thawing-and-freezing as well as drying-and-wetting processes

further increase soil stability (Dexter 1988), additional factors are the presence of organic matter, biological processes, and the consequences of anthropogenic impacts (Dexter 1988; Horn et al. 2019). Horn et al. 1994 stated that  $\sigma_{pc}$  in a homogeneous substrate corresponds to the effective stress as a function of pore water pressure. In a structurally unstable soil, the previous highest hydraulic stress (most negative pore water pressure) affects  $\sigma_{pc}$  (Mosaddeghi et al. 2003).

In loam we found a positive correlation between  $\rho_b$  and  $\sigma_{pc}$  (Fig. 4a), which is in accordance with An et al. (2015) and Mosaddeghi et al. (2003). Rücknagel et al. (2007) used  $\rho_b$  and aggregate density as input for multiple linear regression to estimate  $\sigma_{pc}$  and revealed that an increase in  $\rho_b$  results in higher  $\sigma_{pc}$ . According to Lebert and Horn (1991) with an increment in aggregation caused by a higher clay content, the importance of  $\rho_b$  as determining factor for soil strength decreases. Interestingly, in the present study no significant correlation between  $\rho_b$  and  $\sigma_{pc}$  existed for sand. We noted that the sand samples were in fact very unstable from the beginning. According to Dexter (1988), one of the critical issues of soil stability is its ability to resist the influence of water. During sample preparation in our study (saturation to a standard  $\Psi_m$ ), sand samples consolidated considerably and lost on average 1.72 mm of their initial height. This led to an unavoidable stabilisation of these samples with a mean decline in  $\rho_b$  of  $0.11 \text{ g cm}^{-3}$ , a decrease in  $C_s$  and  $C_c$ , and an increase of  $\sigma_{pc}$  compared to actual field conditions.

The compressibility of loam was higher compared to sand both along the virgin compression range ( $C_c$ ) (Fig. 8a, b) and the recompression range ( $C_s$ ) (Fig. 8c, d). This resulted in more defined curves in loam, whereas low initial void ratios and their weak decline during compression dominated in sand, which is in agreement with Gregory et al. (2006). The sand with its single grain structure showed only little potential to be compressed as the majority of grains were of similar size and the pore system dominated by primary pores. This resulted in a relatively small pore volume that could be compressed, with few soil particles that were small enough to occupy these pore spaces. This is in contrast to the loam with a higher variety of pore sizes as well as of particle sizes leading to greater compressibility. The small ranges of compressibility in sand reflect the low structural development in this substrate as opposed to loam. Low initial void

ratios resulted in higher resistance to compression and therefore decreasing  $C_c$  and  $C_s$  and higher  $\sigma_{pc}$  as higher number of particle contacts lead to increased frictional forces, less available pore space and more energy necessary to relocate water during compression if the initial void ratio is low. This is in accordance with a study by Keller et al. (2011) that revealed initial void ratio as a determining factor for  $\sigma_{pc}$ ,  $C_c$ , and  $C_s$ . Keller et al. (2011) further argued that using a semi-logarithmic curve as basis for calculating soil compression properties has a major impact on these values. However, as it is considered and accepted as the common approach it was also applied here.

In loam,  $\rho_b$  was negatively correlated with  $C_c$  and  $C_s$ ; the corresponding correlations in sand were weaker than we expected as compressibility had already been reduced due to consolidation (Fig. 4) as discussed above. A negative correlation between  $\rho_b$  and  $C_c$  for two agricultural soils was reported by An et al. (2015).

EI was higher in sand than in loam which at first glance seems to be an unexpected result. However, EI was based on a final un-loading step after maximum loading of 575 kPa. The EI relates the changes in void ratio of this final step to the overall changes in void ratio of the entire curve, which were much higher in loam compared to sand. Therefore, absolute void ratio changes in the unloading step were in fact higher in loam than in sand, but the resulting ratio, i.e., the EI, was lower.

#### Spatial and temporal development of bulk soil mechanical properties

We hypothesized structural development to be higher at 14 cm than in 34 cm depth, because closer to the soil surface the influence of environmental factors associated with more intensive wetting and drying can be expected to be stronger. Anyhow, in our study, differences between depths were not very pronounced and only occurred for sand, where  $\rho_b$  was lower at 34 cm depth and  $C_s$  in loam with higher values at lower depth. Rain was scarce in both years and as the bottom of the plots (1 m) was filled with a 25 cm gravel layer with a drainage textile placed on top, plants could not access water from below the plots but depended on precipitation alone. Both the effects of precipitation and drought start from the top thus increasing the variability of  $\Psi_m$  in the topsoil layer



resulting in differences in wetting-and-drying cycles according to depth (Jorda et al. [submitted](#)).

The temporal development was more prominent than the spatial ones. A general setting of soil could be observed with higher  $\rho_b$  in 2020 compared to 2019 in loam, which is not surprising regarding the substrates had been filled-in homogeneously. In loam  $\sigma_{pc}$  increased and  $C_c$  decreased with time.  $\sigma_{pc}$  and  $C_c$  values in the same loam in a lab experiment employing remoulded samples (Roskopf et al. [2022](#)), which can be considered analogous to initial field conditions of the current experiment, fit in well with this timeline. The potential for further compaction, i.e., reduction of the pore space, had already been greatly reduced in sand in 2020, which becomes evident when looking at the extremely narrow ranges of  $C_c$ . Together with declining  $C_s$  in both substrates, this coincides with higher root length densities in all treatments in 2020 compared to 2019 (Vetterlein et al. [2022](#)). Increased root length densities bring about a stabilization of structure, hence higher  $\sigma_{pc}$  and lower  $C_c$  and  $C_s$ . This corresponds to the declining relevance of  $\rho_b$  for the bulk soil mechanical parameters and the decreased correlations between them. The general development of correlations regarding bulk soil measurements getting weaker and less significant over time, points to a diversification of explanatory variables.

#### Required energy and penetration resistances

It is commonly known that decreasing  $\Psi_m$  leads to an increase in forces needed for soil penetration (Quang et al. [2012](#); Elbanna and Witney [1987](#); Wang et al. [2016](#)). The wettest samples displayed no differences between treatments for substrate and genotype, whereas differences according to substrate were more pronounced at lower  $\Psi_m$  as PR responds stronger to  $\Psi_m$  at higher clay contents (Costantini [1996submitted](#)). With the current experimental set-up, it was not possible to me). Both sampling years were very dry, with cumulative precipitation amounts of 180 mm in 2019 and 210 mm in 2020 from sowing until sampling at BBCH83 (German Meteorological Service [2021](#)). This resulted in low soil moistures dropping even below the permanent wilting point (Jorda et al. assure PR at soil moistures around the permanent wilting point in loam, as the penetrometer needle did not resist the occurring forces. In order to be able to tackle this problem in the future, we are

presently working on a comparison of a 1 mm and a 2 mm diameter needle, which will allow us to measure PR at drier conditions and relate the results to the ones obtained so far. Nevertheless, the few measurements that were made in air-dry loam give us an idea of the resistances the roots encountered in the field. PR values of over 50 MPa were reached in loam in five measurements out of 17. Even in sand average values around 5 MPa were around five times higher compared to measurements done at  $-50$  kPa  $\Psi_m$ . A lab experiment using the same loam yielded energies twice as high at the permanent wilting point compared to  $-50$  kPa  $\Psi_m$  (Roskopf et al. [2022](#)).

When transferring the results to natural root systems, it has to be taken into account that a real root does not grow straight into the soil as the PR needle moves. Natural occurring roots utilize the available pore system following paths of least resistance to avoid compacted regions. Nevertheless, root-soil contact is indispensable for obtaining nutrients and water. Our micro penetrometer approach pays attention to root diameter, and cone angle and employs penetration rates which are low enough to prevent any soil plastic viscous effects that could occur otherwise. The forces exerted at the penetrometer conus are recorded and corrected for the friction at the interface between penetrometer shaft and soil. A recessed shaft would ensure that the measured forces only result from the tip but using such a shaft oftentimes does not entirely prevent soil - depending on its texture and moisture - from getting re-attached to it, which then constitutes an error difficult to quantify. That is why a non-recessed shaft was used, which can be pulled out at insertion speed, thus allowing us to estimate shaft friction at any point in time during the measurement and to correct the original forces with these values. The forces encountered during the tip-wise growth of roots can therefore be accurately represented in our very localized measurements. A major difference between an artificial penetrometer and a naturally elongating root remains: the reduction of friction through the secretion of mucilage and the sloughing of root tip cells. Iijima et al. ([2004](#)) measured a 30% decrease in the resistance a root experiences due to the presence of an intact root cap and the secretion of mucilage. Bengough and McKenzie ([1997](#)) quantified that a pushed maize root experiences about 40% of the resistance a metal probe does, and a growing root 50-100% of the resistance of a pushed root. Keeping

in mind that differences due to frictional aspects exist, we can conclude that with our experimental setup we do get close to what roots potentially experience in the field.

Generally, we have to state that genotype has a more pronounced influence on PR with a tendency to higher PR in WT, as it has on the measured bulk soil mechanical parameters. Within the PR tests, failure is not solely attributable to compression as it is the case for  $\sigma_{pc}$ , but also to tensile strength of aggregates. Factors that lead to aggregation and stabilisation of aggregates, such as deposition of organic matter in the rhizosphere leading to an increase in tensile strength, play a major role on this more local scale. Root hairs can improve a crop's ability to deal with drought stress as Marin et al. (2021) showed with barley genotypes, but their impact on soil mechanical parameters at the field scale has not been considered so far. A tendency to higher energy values could be observed in WT, which was also the genotype with higher root length densities at all depths at BBCH83 (fig. 5 in Vetterlein et al. 2022). Our undisturbed samples were taken within the depth intervals of this project partner, which did not show a pronounced depth gradient, thus enabling us to refer to them directly. In particular, the combination of loam and WT resulted in higher forces compared to the other treatments at more negative  $\Psi_m$ . WT had significantly higher shoot dry weight compared to *rth3* (fig. 3 in Vetterlein et al. 2022) in both years, resulting in higher water demand for WT and subsequently an earlier onset and a more severe drought stress. This process is reflected in the  $\Psi_m$  measurements in sand made by Jorda et al. (submitted). A possible explanation for higher energy values in WT might therefore be both the direct impact of increased rooting and the indirect effect of water depletion through roots.

In the laboratory experiment mentioned above, which employed the same loam and sand (Roskopf et al. 2022), PR and energy were measured at the water contents corresponding to the same  $\Psi_m$  as used here, thus resembling a perfect homogeneous state that might come close to initial field conditions. In the present study, energy values in loam and sand were approximately an order of a magnitude higher than in the lab, indicating a process of structural formation in the field. A further explanation for this can be found in the respective sieving and filling procedures resulting in much more

homogeneous samples in the lab, where substrates were sieved to 1 mm and mixed and filled in in small portions, and in slightly lower  $\rho_b$  compared to the field. Reproducing relationships between PR,  $\rho_b$  and soil moisture in the field with repacked samples in the lab was not possible due to structural variability as shown in a study by Costantini (1996).

In all treatments penetration energy was higher at 14 cm depth as opposed to 34 cm which is in line with our hypothesis of the evolution of structure being more pronounced closer to the soil surface due to environmental factors. We assume the higher soil moisture variability and therefore more frequent drying out processes up to the permanent wilting point (Jorda et al. submitted) to be of major importance in this context. A further aspect might have been higher root length densities at BBCH83 at 14 cm depth in sand in both years and in loam in 2020 (Vetterlein et al. 2022).

Our hypothesis that advancing structural development leads to an increase of required energy over time could not be affirmed, in fact penetration energies for sand decreased from one year to the next, while for loam no changes were observed. With time, differences between the substrates emerged, indicating a stronger structural development in loam, as hypothesized. It seems that in loam areas of higher and of lower resistance have balanced each other out, so that differences between years did not appear. In sand, higher root length densities and non-decomposed roots from the previous year (fig. S2 in Vetterlein et al. 2022) might have contributed to the decrease observed, as roots have a smaller effect on aggregation in sand than they do in loam. Not only the adjusted  $\Psi_m$  but also maximum pre-drying plays an important role for the mechanical strength of soils (Hartge 1986). Precipitation was altogether higher in 2020 and as much less water is needed to fill up the sand plots with their higher  $\rho_b$  and lower porosity compared to the loam plots, this resulted in the sand being wetter in 2020 than in 2019 and compared to loam and brought about the very uniform force-displacement curves in these samples. Wang et al. (2016) observed that with subsequent wetting-and-drying cycles soil structure evolves resulting in higher heterogeneity of strength and a simultaneous decrease of both maximum and overall PR values.

## CONCLUSIONS

The overall effect of genotype on bulk soil mechanical properties considered proved to be negligible, whereas PR might be stronger impacted by roots. Substrate with its implications for soil structure was the determining factor for stability, compressibility, and elasticity in the two years following the establishment of the present field experiment. As expected, stronger changes of soil mechanical parameters could be found in loam as opposed to sand. After only a year, higher  $\sigma_{pc}$  and lower compressibility, especially  $C_s$ , were measured, indicating a stabilisation of structure with time in loam but only marginally in sand, in which measurements showed an altogether more uniform behaviour. The sand proved problematic for our measurements, as it consolidated during saturation, distorting the stress-strain relationship and the resulting parameters. Differences of bulk soil parameters between depths were less pronounced but indicated stronger structural development in the top layer. Regarding energy needed for root growth, higher values were found in loam and partially in WT with stronger differences between substrates in drier conditions. Higher PR in the top layer confirmed our hypothesis of stronger stabilization processes close to the soil surface. Temporal development did not change PR in loam and decreased it in sand. In a further field campaign, an adjusted technical set-up with stronger penetration needles will provide us with more detailed information about PR at drier conditions, also accounting for small-scale heterogeneity of values within samples and including a methodological comparison of 1 mm and 2 mm diameter PR needles. Furthermore, we are evaluating PR values in relation to root length densities in a column experiment using substrates and genotypes as in the present study to give us further insights on the effect of the actual root system on PR.

**Acknowledgements** We would like to thank the working group of Doris Vetterlein at the UFZ Halle for the set-up of the field experiment at the research station in Bad Lauchstädt.

**Authors' contributions** According to CRediT (Contributor Roles Taxonomy):

Conceptualization: Stephan Peth, Daniel Uteau; Formal analysis, Investigation and Visualization: Ulla Roskopf; Funding acquisition and Project administration: Stephan Peth, Daniel Uteau; Supervision and Validation: Stephan Peth; Writing (original draft): Ulla Roskopf; Writing (review & editing): Stephan Peth, Daniel Uteau, Ulla Roskopf

**Funding** Open Access funding enabled and organized by Projekt DEAL. This work was conducted within the framework of the priority program 2089, funded by the Deutsche Forschungsgemeinschaft (DFG, German Research Foundation) – 403627636.

**Data availability** The datasets generated during and/or analysed during the current study are available from the corresponding author on reasonable request.

**Code availability** Not applicable.

## Declarations

**Conflicts of interest/Competing interests** The authors have no competing interests to declare that are relevant to the content of this article.

**Open Access** This article is licensed under a Creative Commons Attribution 4.0 International License, which permits use, sharing, adaptation, distribution and reproduction in any medium or format, as long as you give appropriate credit to the original author(s) and the source, provide a link to the Creative Commons licence, and indicate if changes were made. The images or other third party material in this article are included in the article's Creative Commons licence, unless indicated otherwise in a credit line to the material. If material is not included in the article's Creative Commons licence and your intended use is not permitted by statutory regulation or exceeds the permitted use, you will need to obtain permission directly from the copyright holder. To view a copy of this licence, visit <http://creativecommons.org/licenses/by/4.0/>.

## References

- An J, Zhang Y, Yu N (2015) Quantifying the effect of soil physical properties on the compressive characteristics of two arable soils using uniaxial compression tests. *Soil Tillage Res* 145:216–223. <https://doi.org/10.1016/j.still.2014.09.002>
- Bacq-Labreuil A, Crawford J, Mooney SJ, Neal AL, Ritz K (2019) Phacelia (*Phacelia tanacetifolia* Benth.) affects soil structure differently depending on soil texture. *Plant Soil* 441(1):543–554. <https://doi.org/10.1007/s11104-019-04144-4>
- Barto EK, Alt F, Oelmann Y, Wilcke W, Rillig MC (2010) Contributions of biotic and abiotic factors to soil aggregation across a land use gradient. *Soil Biol Biochem* 42(12):2316–2324. <https://doi.org/10.1016/j.soilbio.2010.09.008>
- Bengough AG, McKenzie BM (1997) Sloughing of root cap cells decreases the frictional resistance to maize (*Zea mays* L.) root growth. *J Exp Bot* 48(4):885–893. <https://doi.org/10.1093/jxb/48.4.885>
- Bengough AG, McKenzie BM, Hallett PD, Valentine TA (2011) Root elongation, water stress, and mechanical impedance: A review of limiting stresses and beneficial

- root tip traits. *J Exp Bot* 62(1):59–68. <https://doi.org/10.1093/jxb/erq350>
- Bodner G, Leitner D, Kaul H-P (2014) Coarse and fine root plants affect pore size distributions differently. *Plant Soil* 380(1–2):133–151. <https://doi.org/10.1007/s11104-014-2079-8>
- Bronick CJ, Lal R (2005) Soil structure and management: A review. *Geoderma* 124(1):3–22. <https://doi.org/10.1016/j.geoderma.2004.03.005>
- Bryk M, Kołodziej B, Słowińska-Jurkiewicz A, Jaroszuk-Sierocińska M (2017) Evaluation of soil structure and physical properties influenced by weather conditions during autumn-winter-spring season. *Soil Tillage Res* 170:66–76. <https://doi.org/10.1016/j.still.2017.03.004>
- Burak E, Quinton JN, Dodd IC (2021) Root hairs are the most important root trait for rhizosphere formation of barley (*Hordeum vulgare*), maize (*Zea mays*) and *Lotus japonicus* (Gifu). *Ann Bot* 128(1):45–57. <https://doi.org/10.1093/aob/mcab029>
- Carminati A, Benard P, Ahmed MA, Zarebanadkouki M (2017) Liquid bridges at the root-soil interface. *Plant Soil* 417(1–2):1–15. <https://doi.org/10.1007/s11104-017-3227-8>
- Casagrande A (1936) The determination of pre-consolidation load and its practical significance. *Int Conf Soil Mech Found Eng*:60–64
- Costantini A (1996) Relationships between cone penetration resistance, bulk density, and moisture content in uncultivated, repacked, and cultivated hardsetting and non-hardsetting soils from the coastal lowlands of South-East Queensland. *N Z J For Sci* 26(3):395–412. <http://citeseerx.ist.psu.edu/viewdoc/download?jsessionid=175CDB05791978E10614B5A1833CC34A?doi=10.1.1.707.6869&rep=rep1&type=pdf>. Accessed 7 Dec 2021
- De Baets S, Denbigh TDG, Smyth KM, Eldridge BM, Welton L, Higgins B, Matyjaszkiewicz A, Meersmans J, Larson ER, Chenchiah IV, Liverpool TB, Quine TA, Grierson CS (2020) Micro-scale interactions between Arabidopsis root hairs and soil particles influence soil erosion. *Commun Biol* 3(1):1–11. <https://doi.org/10.1038/s42003-020-0886-4>
- Denef K, Six J (2005) Clay mineralogy determines the importance of biological versus abiotic processes for macroaggregate formation and stabilization. *Eur J Soil Sci* 56(4):469–479. <https://doi.org/10.1111/j.1365-2389.2004.00682.x>
- Dexter AR (1988) Advances in Characterization of Soil Structure.pdf. *Soil Tillage Res* 11:199–238
- Diel J, Vogel H-J, Schlüter S (2019) Impact of wetting and drying cycles on soil structure dynamics. *Geoderma* 345:63–71. <https://doi.org/10.1016/j.geoderma.2019.03.018>
- Dixon JB (1991) Roles of clays in soils. *Appl Clay Sci* 5(5):489–503. [https://doi.org/10.1016/0169-1317\(91\)90019-6](https://doi.org/10.1016/0169-1317(91)90019-6)
- Elbanna EB, Witney BD (1987) Cone penetration resistance equation as a function of the clay ratio, soil moisture content and specific weight. *J Terramech* 24(1):41–56. [https://doi.org/10.1016/0022-4898\(87\)90058-9](https://doi.org/10.1016/0022-4898(87)90058-9)
- Galloway AF, Akhtar J, Marcus SE, Fletcher N, Field K, Knox P (2020) Cereal root exudates contain highly structurally complex polysaccharides with soil-binding properties. *Plant J* 103(5):1666–1678. <https://doi.org/10.1111/tj.14852>
- German Meteorological Service (2021) [https://opendata.dwd.de/climate\\_environment/](https://opendata.dwd.de/climate_environment/). Accessed 14 Dec 2021
- Gregory AS, Whalley WR, Watts CW, Bird NRA, Hallett PD, Whitmore AP (2006) Calculation of the compression index and precompression stress from soil compression test data. *Soil Tillage Res* 89(1):45–57. <https://doi.org/10.1016/j.still.2005.06.012>
- Grosbellet C, Vidal-Beaudet L, Caubel V, Charpentier S (2011) Improvement of soil structure formation by degradation of coarse organic matter. *Geoderma* 162(1–2):27–38. <https://doi.org/10.1016/j.geoderma.2011.01.003>
- Haichar F e Z, Marol C, Berge O, Rangel-Castro JI, Prosser JI, Balesdent J, Heulin T, Achouak W (2008) Plant host habitat and root exudates shape soil bacterial community structure. *ISME J* 2(12):1221–1230. <https://doi.org/10.1038/ismej.2008.80>
- Hallett P, Feeney D, Bengough A, Rillig M, Scrimgeour C, Young I (2009) Disentangling the impact of AM fungi versus roots on soil structure and water transport. *Plant Soil* 314(1):183–196. <https://doi.org/10.1007/s11104-008-9717-y>
- Han E, Kautz T, Perkins U, Uteau D, Peth S, Huang N, Horn R, Köpke U (2015) Root growth dynamics inside and outside of soil biopores as affected by crop sequence determined with the profile wall method. *Biol Fertil Soils* 51(7):847–856. <https://doi.org/10.1007/s00374-015-1032-1>
- Hartge KH (1986) A concept of compaction. *Z Pflanzenernähr Bodenkd* 149(4):361–370. <https://doi.org/10.1002/jpln.19861490402>
- Horn R, Taubner H, Wuttke M, Baumgartl T (1994) Soil physical properties related to soil structure. *Soil Tillage Res* 30(2):187–216
- Horn R, Holthusen D, Dörner J, Mordhorst A, Fleige H (2019) Scale-dependent soil strengthening processes – What do we need to know and where to head for a sustainable environment? *Soil Tillage Res* 195:104388. <https://doi.org/10.1016/j.still.2019.104388>
- Iijima M, Higuchi T, Barlow PW (2004) Contribution of root cap mucilage and presence of an Intact root cap in maize (*Zea mays*) to the reduction of soil mechanical impedance. *Ann Bot* 94(3):473–477. <https://doi.org/10.1093/aob/mch166>
- ISO (2017) Geotechnical investigation and testing — Laboratory testing of soil — Part 5: Incremental loading oedometer test (ISO 17892-5:2017). Geneva, Switzerland, International Organization for Standardization (ISO). <https://www.iso.org/standard/55247.html>. Accessed 12 Oct 2021
- ISO (2018) Metallic materials — Calibration and verification of static uniaxial testing machines — Part 1: Tension/compression testing machines — Calibration and verification of the force-measuring system (ISO 7500-1:2018). Geneva, Switzerland, International Organization for Standardization (ISO). <https://www.iso.org/standard/72572.html>. Accessed 12 Oct 2021
- Jorda H, Ahmed MA, Javaux M, Carminati A, Duddek P, Vetterlein D, Vanderborght J (submitted) Field scale plant water relation of maize (*Zea mays*) under drought – impact of root hairs and soil texture. *Plant Soil*: submitted 01/04/2022
- Keller T, Lamandé M, Schjønning P, Dexter AR (2011) Analysis of soil compression curves from uniaxial confined



- compression tests. *Geoderma* 163(1–2):13–23. <https://doi.org/10.1016/j.geoderma.2011.02.006>
- Koebnick N, Daly KR, Keyes SD, George TS, Brown LK, Raffan A, Cooper LJ, Naveed M, Bengough AG, Sinclair I, Hallett PD, Roose T (2017) High-resolution synchrotron imaging shows that root hairs influence rhizosphere soil structure formation. *New Phytol* 216(1):124–135. <https://doi.org/10.1111/nph.14705>
- Koebnick N, Daly KR, Keyes SD, Bengough AG, Brown LK, Cooper LJ, George TS, Hallett PD, Naveed M, Raffan A, Roose T (2018) Imaging microstructure of the barley rhizosphere: Particle packing and root hair influences. *New Phytol* 221(4):1878–1889. <https://doi.org/10.1111/nph.15516>
- Lebert M, Horn R (1991) A method to predict the mechanical strength of agricultural soils. *Soil Tillage Res* 19(2–3):275–286. [https://doi.org/10.1016/0167-1987\(91\)90095-F](https://doi.org/10.1016/0167-1987(91)90095-F)
- Leuther F, Schlüter S (2021) Impact of freeze–thaw cycles on soil structure and soil hydraulic properties. *Soil* 7(1):179–191. <https://doi.org/10.5194/soil-7-179-2021>
- Li A, Fahey TJ, Pawlowska TE, Fisk MC, Burtis J (2015) Fine root decomposition, nutrient mobilization and fungal communities in a pine forest ecosystem. *Soil Biol Biochem* 83:76–83. <https://doi.org/10.1016/j.soilbio.2015.01.019>
- Lucas M, Schlüter S, Vogel H-J, Vetterlein D (2019) Roots compact the surrounding soil depending on the structures they encounter. *Sci Rep* 9(1):16236. <https://doi.org/10.1038/s41598-019-52665-w>
- Lucas M, Vetterlein D, Vogel H-J, Schlüter S (2021) Revealing pore connectivity across scales and resolutions with X-ray CT. *Eur J Soil Sci* 72(2):546–560. <https://doi.org/10.1111/ejss.12961>
- Marin M, Feeney DS, Brown LK, Naveed M, Ruiz S, Koebnick N, Bengough AG, Hallett PD, Roose T, Puértolas J, Dodd IC, George TS (2021) Significance of root hairs for plant performance under contrasting field conditions and water deficit. *Ann Bot* 128(1):1–16. <https://doi.org/10.1093/aob/mcaa181>
- Meier U, Biologische Bundesanstalt für Land- und Forstwirtschaft (1997) Growth stages of mono- and dicotyledonous plants: BBCH-Monograph. Blackwell Wissenschafts-Verlag. <https://www.julius-kuehn.de/media/Veroeffentlichungen/bbch%20epa%20en/page.pdf>. Accessed 10 Oct 2021
- Mosaddeghi MR, Hemmat A, Hajabbasi MA, Alexandrou A (2003) Pre-compression stress and its relation with the physical and mechanical properties of a structurally unstable soil in central Iran. *Soil Tillage Res* 70(1):53–64
- Naveed M, Moldrup P, Vogel H-J, Lamandé M, Wildenschild D, Tuller M, de Jonge LW (2014) Impact of long-term fertilization practice on soil structure evolution. *Geoderma* 217–218:181–189. <https://doi.org/10.1016/j.geoderma.2013.12.001>
- Naveed M, Brown LK, Raffan AC, George TS, Bengough AG, Roose T, Sinclair I, Koebnick N, Cooper L, Hackett CA, Hallett PD (2017) Plant exudates may stabilize or weaken soil depending on species, origin and time: Effect of plant exudates on rhizosphere formation. *Eur J Soil Sci* 68(6):806–816. <https://doi.org/10.1111/ejss.12487>
- Nuccio EE, Starr E, Karaoz U, Brodie EL, Zhou J, Tringe SG, Malmstrom RR, Woyke T, Banfield JF, Firestone MK, Pett-Ridge J (2020) Niche differentiation is spatially and temporally regulated in the rhizosphere. *ISME J* 14(4):999–1014. <https://doi.org/10.1038/s41396-019-0582-x>
- Nunan N, Leloup J, Ruamps LS, Pouteau V, Chenu C (2017) Effects of habitat constraints on soil microbial community function. *Sci Rep* 7(1):4280. <https://doi.org/10.1038/s41598-017-04485-z>
- Oades JM (1993) The role of biology in the formation, stabilization and degradation of soil structure. *Geoderma* 56(1–4):377–400. [https://doi.org/10.1016/0016-7061\(93\)90123-3](https://doi.org/10.1016/0016-7061(93)90123-3)
- Oleghe E, Naveed M, Baggs EM, Hallett PD (2017) Plant exudates improve the mechanical conditions for root penetration through compacted soils. *Plant Soil* 421(1–2):19–30. <https://doi.org/10.1007/s11104-017-3424-5>
- Peth S, Rostek J, Zink A, Mordhorst A, Horn R (2010) Soil testing of dynamic deformation processes of arable soils. *Soil Tillage Res* 106(2):317–328. <https://doi.org/10.1016/j.still.2009.10.007>
- Pett-Ridge J, Firestone MK (2017) Using stable isotopes to explore root-microbe-mineral interactions in soil. *Rhizosphere* 3:244–253. <https://doi.org/10.1016/j.rhisph.2017.04.016>
- Phalempin M, Lippold E, Vetterlein D, Schlüter S (2021) Soil texture and structure heterogeneity predominantly governs bulk density gradients around roots. *Vadose Zone J* 20(5). <https://doi.org/10.1002/vzj2.20147>
- Pihlap E, Vuko M, Lucas M, Steffens M, Schloter M, Vetterlein D, Enderich M, Kögel-Knabner I (2019) Initial soil formation in an agriculturally reclaimed open-cast mining area—The role of management and loess parent material. *Soil Tillage Res* 191:224–237. <https://doi.org/10.1016/j.still.2019.03.023>
- Quang PV, Jansson P, Khoa LV (2012) Soil penetration resistance and its dependence on soil moisture and age of the raised-beds in the Mekong Delta, Vietnam. *Int J Eng Res Dev* 4(8):84–93. <https://www.semanticscholar.org/paper/Soil-Penetration-Resistance-and-Its-Dependence-on-QuangJansson/994c2b435e39aaf7d226f2f8b6ee907142a973b7>. Accessed 21 Oct 2021
- Roskopf U, Uteau D, Peth S (2022) Effects of mucilage concentration at different water contents on mechanical stability and elasticity in a loamy and a sandy soil. *Eur J Soil Sci*. <https://doi.org/10.1111/ejss.13189>
- RStudio Team (2020) RStudio: Integrated Development Environment for R. RStudio, PBC, Boston, MA. <http://www.rstudio.com/>. Accessed 3 Nov 2021
- Rücknagel J, Hofmann B, Paul R, Christen O, Hulsbergen K-J (2007) Estimating precompression stress of structured soils on the basis of aggregate density and dry bulk density. *Soil Tillage Res* 92(1–2):213–220. <https://doi.org/10.1016/j.still.2006.03.004>
- Ruiz S, Schymanski, S. J., & Or, D. (2017). Mechanics and Energetics of Soil Penetration by Earthworms and Plant Roots: Higher Rates Cost More. *Vadose Zone J*, 16(8), 0. <https://doi.org/10.2136/vzj2017.01.0021>
- Schon NL, Mackay AD, Gray RA, van Koten C, Dodd MB (2017) Influence of earthworm abundance and diversity on soil structure and the implications for soil services throughout the season. *Pedobiologia* 62:41–47. <https://doi.org/10.1016/j.pedobi.2017.05.001>

- Vetterlein D, Lippold E, Schreiter S, Phalempin M, Fahrenkamp T, Hochholdinger F, Marcon C, Tarkka M, Oburger E, Ahmed M, Javaux M, Schlüter S (2021) Experimental platforms for the investigation of spatiotemporal patterns in the rhizosphere—Laboratory and field scale. *J Plant Nutr Soil Sci* 184(1):35–50. <https://doi.org/10.1002/jpln.202000079>
- Vetterlein D, Phalempin M, Lippold E, Schlüter S, Schreiter S, Ahmed MA, Carminati A, Duddek P, Jorda H, Bienert P, Bienert D, Tarkka M, Ganther M, Oburger E, Santangeli M, Javaux M, Vanderborght J (2022) Root hairs matter at field scale for maize shoot growth and nutrient uptake, but root trait plasticity is primarily triggered by texture and drought. *Plant Soil Spec Issue S90*. <https://doi.org/10.21203/rs.3.rs-1277067/v1>
- Wang D-Y, Tang C-S, Cui Y-J, Shi B, Li J (2016) Effects of wetting–drying cycles on soil strength profile of a silty clay in micro-penetrometer tests. *Eng Geol* 206:60–70. <https://doi.org/10.1016/j.enggeo.2016.04.005>
- Wang ZH, Fang H, Chen M (2017) Effects of root exudates of woody species on the soil anti-erodibility in the rhizosphere in a karst region, China. *PeerJ* 5:e3029. <https://doi.org/10.7717/peerj.3029>
- Wickham H (2016) *ggplot2: Elegant Graphics for Data Analysis*. Springer-Verlag, New York. <https://ggplot2.tidyverse.org>. Accessed 3 Nov 2021

**Publisher's note** Springer Nature remains neutral with regard to jurisdictional claims in published maps and institutional affiliations.